J|A|C|S ARTICLES

Published on Web 08/20/2010

Shared Biosynthesis of the Saliniketals and Rifamycins in *Salinispora arenicola* is Controlled by the *sare1259*-Encoded Cytochrome P450

Micheal C. Wilson,[†] Tobias A. M. Gulder,[†] Taifo Mahmud,[‡] and Bradley S. Moore*[,†,§]

Center for Marine Biotechnology and Biomedicine, Scripps Institution of Oceanography, University of California at San Diego, La Jolla, California 92093-0204, Department of Pharmaceutical Sciences, Oregon State University, Corvallis, Oregon 97331, and The Skaggs School of Pharmacy and Pharmaceutical Sciences, University of California at San Diego, La Jolla, California 92093

Received July 4, 2010; E-mail: bsmoore@ucsd.edu

Abstract: Saliniketals A and B are unusual polyketides from the marine actinomycete *Salinispora arenicola* that inhibit ornithine decarboxylase induction. The structural similarities between the saliniketals and the ansa chain of the potent rifamycin antibiotics, which co-occur in the fermentation broth, suggest a common origin between the two compound classes. Using PCR-directed mutagenesis, chemical complementation studies, and stable isotope feeding experiments, we showed that the saliniketals are byproducts of the rifamycin biosynthetic pathway diverging at the stage of 34a-deoxyrifamycin W. Our results suggest that a single enzyme, the cytochrome P450 monooxygenase encoded by *sare1259*, catalyzes multiple oxidative rearrangement reactions on 34a-deoxyrifamyin W to yield both the saliniketal and rifamycin structural classes.

Introduction

Saliniketals A (**1**) and B (**2**), originally isolated by Fenical and co-workers in 2007, are novel bicyclic polyketides produced by the obligate marine actinomycete *Salinispora arenicola* (Figure 1).[1] These inhibitors of ornithine decarboxylase induction,[1] an effective treatment strategy for cancer chemoprevention,[2] harbor unusual structural features that have inspired three total syntheses to date.[3−5] The saliniketals contain an unprecedented 1,4-dimethyl-2,8-dioxabicyclo[3.2.1]octane ring system with a polyketide side chain at C11 that terminates in a primary amide. The global structure of **1** and **2** is also notable because of the striking similarity, including the exact stereochemistry, to the ansa chain of the potent rifamycin antibiotics (**3**−**6**), which co-occur in the fermentation broth (Figure 1).[1] While the rifamycin polyketides are assembled from the aromatic starter unit 3-amino-5-hydroxybenzoic acid (AHBA) with two acetate and eight propionate extender units,[6] the presence of the primary amide on the saliniketals originally suggested that they were neither biosynthetic shunt products nor degradation products of rifamycin because cleavage of the C−N bond of the AHBA-derived aromatic starter unit was unlikely.[1] Instead, the saliniketals were proposed to originate from a three-carbon starter unit that is extended by a disparate polyketide synthase (PKS)

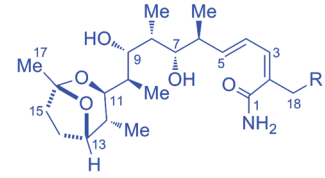

1 Saliniketal A R=H
2 Saliniketal B R= OH

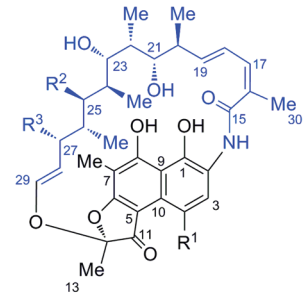

		R^1	R^2	R^3
3	Rifamycin B	OCH_2CO_2H	$OCOCH_3$	OCH_3
4	Rifamycin SV	OH	$OCOCH_3$	OCH_3
5	DMRSV	OH	$OCOCH_3$	OH
6	DMDARSV	OH	OH	OH

Figure 1. Structures of the saliniketals (**1**−**2**) and rifamycins (**3**−**6**) from *S. arenicola* CNS-205. The numbering of **1**−**6** is consistent with prior publications.[1,42]

[†] Scripps Institution of Oceanography, University of California at San Diego.
[‡] Oregon State University.
[§] The Skaggs School of Pharmacy and Pharmaceutical Sciences, University of California at San Diego.

(1) Williams, P.; Asolkar, R.; Kondratyuk, T.; Pezzuto, J.; Jensen, P.; Fenical, W. *J. Nat. Prod.* **2007**, *70*, 83.
(2) Pegg, A.; Shantz, L.; Coleman, C. *J. Cell. Biochem.* **1995**, *59*, 132.
(3) Liu, J.; De Brabander, J. K. *J. Am. Chem. Soc.* **2009**, *131*, 12562.
(4) Paterson, I.; Razzak, M.; Anderson, E. A. *Org. Lett.* **2008**, *10*, 3295.
(5) Yadav, J. S.; Hossain, S. S.; Madhu, M.; Mohapatra, D. K. *J. Org. Chem.* **2009**, *74*, 8822.
(6) Floss, H. G.; Yu, T. W. *Chem. Rev.* **2005**, *105*, 621.

with two acetate and five propionate units to form the ketide with the exact stereochemistry as in **3**−**6**.[1] However, prior to this study, this hypothesis had not been explored experimentally.

The rifamycins were first identified by Sensi and co-workers in 1959 from a terrestrial actinomycete that would eventually be classified as *Amycolatopsis mediterranei*.[6,7] In 2006, Kim et al. first reported the production of rifamycins B (**3**) and SV (**4**) from a strain of *Salinispora* isolated from an Australian marine sponge.[8] Later, Jensen and co-workers showed that the *Salinispora* exhibit species-specific secondary metabolite production trends in which saliniketal and unspecified rifamycins along with the staurosporines were observed in all examined strains of *S. arenicola*, thus comprising the *S. arenicola* core chemotype.[9] Bioinformatic analysis of the Palauan *S. arenicola* CNS-205 genome and polymerase chain reaction (PCR) based screening experiments confirmed genes predicted to be involved in the biosynthesis of rifamycins.[8,10] The high sequence identity between genes in the *S. arenicola* rifamycin cluster (SA-*rif*) and genes from the well characterized *A. mediterranei* S699 rifamycin biosynthetic gene cluster (AM-*rif*) suggests that the *rif* locus has undergone horizontal gene transfer.[10]

In the present study, we explored the biosynthetic relationship between the rifamycins and saliniketals by a multidisciplinary approach involving bioinformatic analysis, *in vivo* mutagenesis, chemical complementation, and stable isotope incorporation studies. In doing so, we probed the following questions: Does the structural similarity between the saliniketals and rifamycins originate from a common biosynthetic machinery? If so, are the saliniketals shunt products of the rifamycin polyketide assembly or molecules selectively generated from a rifamycin-type biosynthetic precursor by a distinct enzyme in the pathway? Herein we report that the saliniketals are unexpected products of the central *rif* pathway intermediate 34a-deoxyrifamycin W (**7**; see Figure 4) in which the cytochrome P450 monooxygenase (CYP) Sare1259 is responsible for dual oxidative rearrangement reactions that lead to the formation of the mature rifamycins **3**−**6** and the truncated saliniketals **1**−**2**.

Results

Chemical Analysis of *S. arenicola* CNS-205 and *A. mediterranei* S699. Organic extracts of *S. arenicola* CNS-205 and *A. mediterranei* S699 were analyzed by liquid chromatography/mass spectrometry (LC/MS) to directly compare their *rif* chemistry with known saliniketal and rifamycin chemical standards. In addition to **1** and **2**, *S. arenicola* CNS-205 produces a mixture of rifamycin SV (**4**), 27-*O*-demethyl-25-*O*-desacetylrifamycin SV (**5**) and 27-*O*-demethylrifamycin SV (**6**) when cultured in A1 production media (Figure 1). *Amycolatopsis mediterranei* S699, on the other hand, primarily produces rifamycin B (**3**).[11] After a closer inspection of extracts from the fermentation broth of *A. mediterranei* S699 grown in YMG liquid media, we learned that **1** and **2** are not unique to *S. arenicola* but are also minor components of the original rifamycin producer (Figure S1, Supporting Information). The coproduction of both compound classes by these distantly related actinomycetes suggested that the saliniketals and rifamycins may arise from a common biosynthetic pathway.

Bioinformatic Analysis of the *S. arenicola* CNS-205 Genome. In early 2007, the completion of the *S. arenicola* CNS-205 genome sequencing project yielded a 5 786 361 bp genome (CP000850) with at least 30 distinct secondary metabolite gene clusters.[10] Initially excluding the rifamycin biosynthetic gene cluster (SA-*rif*), none of the remaining 12 polyketide synthase (PKS)-associated pathways had a domain architecture consistent with the predicted assembly of the saliniketals. We therefore were left with no other viable option but the 92 kb SA-*rif* cluster for saliniketal biosynthesis. The SA-*rif* pathway is comprised of 39 open reading frames (ORFs), 33 of which are homologous to genes in the AM-*rif* cluster with identities >50% (Table 1). The SA-*rif* cluster is organized similarly to the AM-*rif* cluster with a distinct 10 module PKS operon (*rifA-E)*, an AHBA biosynthetic subcluster, and a 24 kb tailoring and regulation region (Figure 2). All genes determined essential for the biosynthesis of rifamycin B in *A. mediterranei* S699 share a homologue in the SA-*rif* cluster.[6,12−17] There are, however, ten genes in the tailoring region of the AM-*rif* cluster that do not have homologues in the SA-*rif* cluster (*rifO*, *rif-orf2*, *rifP*, *rifQ*, *rif-orf3*, *rif-orf4*, *rif-orf8*, *rif-orf11*, *rif-orf17*, and *rif-orf37*), and conversely, the SA-*rif* cluster contains six genes without counterparts in AM-*rif* (*sare1240*, *sare1241*, *sare1258*, *sare1261*, *sare1276*, and *sare1278*). The unique *S. arenicola* genes are annotated as a multicopper oxidase (*sare1241*), a Rieske-domain protein (*sare1258*), a FAD-dependent oxidoreductase (*sare1278*), two hypothetical proteins (*sare1240* and *sare1276*), and a ferrodoxin-domain containing protein (*sare1261*). The regions upstream and downstream of the SA-*rif* locus also differ from the AM-*rif* cluster in that none of the transport, membrane protein, ribosomal protein, or RNA polymerase genes are shared. Homologues of many of these genes are, however, located elsewhere in the *S. arenicola* genome (data not shown). Interestingly, SA and AM *rif* share genes related to aminodeoxysugar biosynthesis (*sare1263*−*7* corresponding to *rif-orf7*, *rif-orf6*, *rif-orf9*, *rif-orf10*, and *rif-orf18*, respectively) while no glycosylated rifamycins have been reported from either strain. The coproduction of the closely related glycosylated compound, tolypomycin Y, with rifamycins B (**3**) and O by *Amycolatopsis tolypomycina*[18] suggests that these genes may be silent in SA-*rif*, as proposed for the aminodeoxysugar locus in AM-*rif*.[19]

Inactivation of the AHBA Synthase (*rifK*) and the Transketolase (*rif-orf15*). The bioinformatic analysis of the SA and AM *rif* clusters did not support the previously proposed mechanism

(7) Sensi, P.; Margalith, P.; Timbal, M. *Farmaco Ed. Sci.* **1959**, *14*, 146.
(8) Kim, T. K.; Hewavitharana, A. K.; Shaw, P. N.; Fuerst, J. A. *Appl. Environ. Microbiol.* **2006**, *72*, 2118.
(9) Jensen, P. R.; Williams, P. G.; Oh, D. C.; Zeigler, L.; Fenical, W. *Appl. Environ. Microbiol.* **2007**, *73*, 1146.
(10) Penn, K.; Jenkins, C.; Nett, M.; Udwary, D. W.; Gontang, E. A.; McGlinchey, R. P.; Foster, B.; Lapidus, A.; Podell, S.; Allen, E. E.; Moore, B. S.; Jensen, P. R. *ISME J.* **2009**, *3*, 1193.
(11) Kim, C. G.; Kirschning, A.; Bergon, P.; Zhou, P.; Su, E.; Sauerbrei, B.; Ning, S.; Ahn, Y.; Breuer, M.; Leistner, E.; Floss, H. G. *J. Am. Chem. Soc.* **1996**, *118*, 7486.
(12) Floss, H.; Yu, T. *Curr. Opin. Chem. Biol.* **1999**, *3*, 592.
(13) Xu, J.; Wan, E.; Kim, C. J.; Floss, H. G.; Mahmud, T. *Microbiology* **2005**, *151*, 2515.
(14) Yu, T.; Muller, R.; Muller, M.; Zhang, X.; Draeger, G.; Kim, C.; Leistner, E.; Floss, H. *J. Biol. Chem.* **2001**, *276*, 12546.
(15) Yu, T. W.; Shen, Y.; Doi-Katayama, Y.; Tang, L.; Park, C.; Moore, B. S.; Richard Hutchinson, C.; Floss, H. G. *Proc. Natl. Acad. Sci. U.S.A.* **1999**, *96*, 9051.
(16) Xiong, Y.; Wu, X.; Mahmud, T. *ChemBioChem* **2005**, *6*, 834.
(17) Xu, J.; Mahmud, T.; Floss, H. G. *Arch. Biochem. Biophys.* **2003**, *411*, 277.
(18) Kishi, T.; Yamana, H.; Muroi, M.; Harada, S.; Asai, M. *J. Antibiot. (Tokyo)* **1972**, *25*, 11.
(19) August, P. R.; Tang, L.; Yoon, Y. J.; Ning, S.; Müller, R.; Yu, T.-W.; Taylor, M.; Hoffmann, D.; Kim, C.-G.; Zhang, X.; Hutchinson, C. R.; Floss, H. G. *Chem. Biol.* **1998**, *5*, 69.

Table 1. Summary of SA-*rif* Cluster and Chemotypes of Genetically Mutated Strains

SA-*rif* gene	annotation	AM-*rif* homologue	% identity	chemotype of mutant
Sare_1240	hypothetical protein	N/A	N/A	
Sare_1241	multicopper oxidase type 2	N/A	N/A	
Sare_1242[a]	oxidoreductase domain protein	*rifS*	76	no production of **1**−**8**
Sare_1243[a]	oxidoreductase domain protein	*rifT*	57	no production of **1**−**8**
Sare_1244	hypothetical protein	*orf35*	59	
Sare_1245[a]	cytochrome P450	*orf0*	82	no production of **1**−**8**
Sare_1246	AMP-dependent synthetase and ligase	*rifA*	72	
Sare_1247	beta-ketoacyl synthase	*rifB*	73	
Sare_1248	beta-ketoacyl synthase	*rifC*	71	
Sare_1249	beta-ketoacyl synthase	*rifD*	69	
Sare_1250	acyltransferase	*rifE*	72	
Sare_1251	*N*-acetyltransferase	*rifF*	68	
Sare_1252	hypothetical protein	*orf1*	50	
Sare_1253	3-dehydroquinate synthase	*rifG*	79	
Sare_1254	3-deoxy-7-phosphoheptulonate synthase	*rifH*	66	
Sare_1255[a]	AHBA synthase	*rifK*	86	no production of **1**−**8**
Sare_1256	oxidoreductase domain protein	*rifL*	79	
Sare_1257	putative phosphatase	*rifM*	83	
Sare_1258	rieske [2Fe-2S] domain protein	N/A	N/A	
Sare_1259[a]	cytochrome P450	*orf5*	71	**7**
Sare_1260[a]	cytochrome P450	*orf16*	73	WT
Sare_1261	protein of unknown function DUF1271	N/A	N/A	
Sare_1262[a]	acetyltransferase, PapA5	*orf20*	58	**1**, **2**, and **6**
Sare_1263[a]	protein of unknown function DUF1205	*orf7*	66	WT
Sare_1264[a]	DegT/DnrJ/EryC1/StrS aminotransferase	*orf6*	86	WT
Sare_1265[a]	aminotransferase class-III	*orf9*	79	WT
Sare_1266[a]	oxidoreductase domain protein	*orf10*	70	WT
Sare_1267[a]	NDP-hexose 2,3-dehydratase	*orf18*	79	WT
Sare_1268	monooxygenase FAD-binding	*orf19*	74	
Sare_1269	type II thioesterase	*rifR*	70	
Sare_1270	regulatory protein LuxR	*orf36*	64	
Sare_1271	methyltransferase type 11	*orf14*	65	
Sare_1272[a]	transketolase domain protein	*orf15A*	80	no production of **1**−**8**
Sare_1273[a]	transketolase central region	*orf15B*	70	no production of **1**−**8**
Sare_1274[a]	shikimate dehydrogenase	*rifI*	55	WT
Sare_1275	ROK family protein	*rifN*	53	
Sare_1276	DoxX family protein	N/A	N/A	
Sare_1277	3-dehydroquinate dehydratase	*rifJ*	77	
Sare_1278	FAD-dependent oxidoreductase	N/A	N/A	

[a] Genes were inactivated in this study. Abbreviation: (WT) wild-type chemistry observed (compounds **1**−**2** and **4**−**6**).

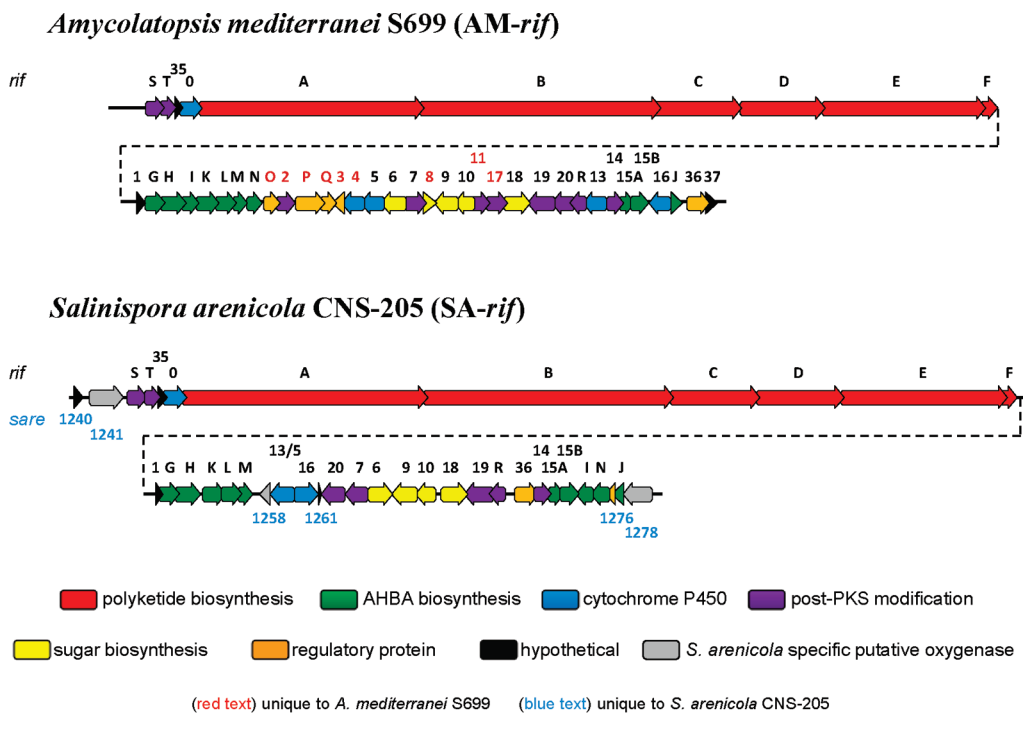

Figure 2. Comparison of the rifamycin biosynthetic gene clusters from *A. mediterranei* S699 (AF040571) and *S. arenicola* CNS-205 (CP000850).

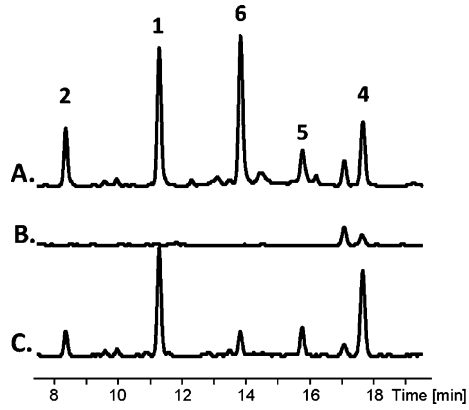

Figure 3. HPLC-MS analysis of the inactivation of the *S. arenicola* AHBA synthase (*rifK, sare1255*) and chemical complementation of resulting mutant (*rifK::apr*^{R}). Extracted ion chromatogram (EIC) for masses corresponding to the *m/z* of the sodium adducts of the saliniketals (**1**−**2**) and rifamycins (**4**−**6**) from *Salinispora arenicola* (A) wild-type, (B) *rifK::apr*^{R}, and (C) *rifK::apr*^{R} mutant chemically complemented with synthetically prepared AHBA (25 mM).

for saliniketal formation involving a distinct three-carbon primer unit intercepting the rifamycin synthase in lieu of the aromatic precursor AHBA. Since the saliniketals are not unique to *S. arenicola* and are also produced by *A. mediterranei*, we explored the biosynthetic scenario that the saliniketals are directly related to the rifamycins as either shunt or degradative products. In order to initially probe their putative biosynthetic relationship, we employed a PCR-directed gene replacement methodology to disrupt the AHBA synthase encoding gene *rifK* (*sare1255*) with an apramycin resistance cassette (*acc(3)IV*) as described previously for cyclomarin biosynthesis in *S. arenicola*.[20] As predicted, inactivation of *rifK* in *S. arenicola* completely abolished the production of all rifamycins. In addition, the saliniketals were also not produced in the *rifK* mutant (*rifK::apr*^{R}), providing unequivocal evidence that these natural products share a common biosynthetic origin from AHBA (Figure 3A−B). This conclusion was further substantiated through the successful chemical complementation of *rifK::apr*^{R} with synthetically prepared AHBA that restored both saliniketal (**1**−**2**) and rifamycin (**3**−**6**) production to wild-type levels (Figure 3C). Similar results were also observed when we inactivated, with a single replacement, the SA-*rif* transketolase A (*sare1272*) and B (*sare1273*) subunits corresponding to *rif-orf15A* and *rif-orf15B* from AM-*rif*, respectively (Figure S2, Supporting Information). Based on in vitro reconstitution of genes involved in AHBA biosynthesis with the *E. coli* transketolase (*tktA*),[21] Orf15 is predicted to catalyze the conversion of 3-amino-3-deoxy-D-fructose-6-phosphate to imino-erythrose-4-phosphate during the biosynthesis of AHBA.[21−23] To the best of our knowledge, these are the first experimental data to confirm the function of Orf15 in vivo.

To explore whether the nitrogen atom of saliniketal's primary amide originates from AHBA or from an alternate source, we synthesized and then administered [^{15}N]AHBA to production cultures of the rifamycin deficient mutant *rifK::apr*^{R}. We

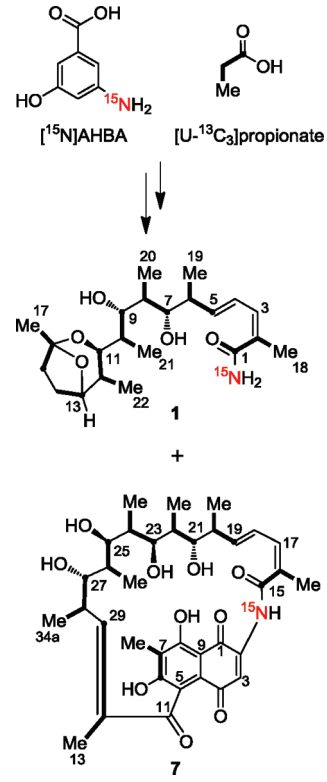

Figure 4. Stable isotope labeling pattern observed for **1** and proposed for **7** (see ref 43) from the incorporation of [^{15}N]AHBA and [U-$^{13}C_3$]propionate.

observed by MS similar isotopic enrichments of the saliniketal and rifamycin biosynthetic products as in the synthetic [^{15}N]AHBA precursor of 25 atom % ^{15}N, thereby confirming that the primary amide nitrogen of the saliniketals is derived from the "unlikely"[1] C−N bond cleavage of the AHBA unit (Figure 4). These observations also suggested that **1** and **2** are not shunt products formed during polyketide extension but rather originate from a mature rifamycin macrocyclic product since the priming AHBA nitrogen atom ultimately resides at the terminating carbonyl C1 group of saliniketal.

Identification of Genes Directly Involved in Saliniketal Production. Once we established that **1**−**6** share a single post-PKS assembly biosynthetic precursor, we methodically inactivated genes in the SA-*rif* cluster with homologous representatives in AM-*rif* to determine which are involved with the production of **1** and **2** and to elucidate the point at which the rifamycin and saliniketal pathways diverge. We inactivated four genes with predicted functions based on characterization or inactivation of their corresponding AM-*rif* homologues (*sare1245*, *sare1259*, *sare1260*, and *sare1262* corresponding to *rif-orf0*, *rif-orf13/rif-orf5*, *rif-orf16*, and *rif-orf20*, respectively).

We first explored *rif-orf20*, which encodes an acetyltransferase that catalyzes the acetylation of the C25 hydroxyl of **6** to form **5**.[16] Based on an early mechanistic proposal for the formation of **1**, we envisioned the assimilation of the 25-O-acetyl unit of **4** or **5** into the bicyclic ring of **1** at C16/C17. Deletion of *sare1262* yielded a mutant that accumulated the desacetylated **6** without any effect on the production of **1** and **2**, suggesting that the pathways must diverge prior to the formation of **6**. This result was corroborated through an isotope experiment with [U−$^{13}C_3$]propionate that enriched **1** with six intact propionate units and one incomplete propionate unit at C13/C14 (Figure 4) corresponding to the formal loss of C34a

(20) Schultz, A. W.; Oh, D. C.; Carney, J. R.; Williamson, R. T.; Udwary, D. W.; Jensen, P. R.; Gould, S. J.; Fenical, W.; Moore, B. S. *J. Am. Chem. Soc.* **2008**, *130*, 4507.
(21) Guo, J.; Frost, J. W. *J. Am. Chem. Soc.* **2002**, *124*, 528.
(22) Arakawa, K.; Muller, R.; Mahmud, T.; Yu, T. W.; Floss, H. G. *J. Am. Chem. Soc.* **2002**, *124*, 10644.
(23) Guo, J.; Frost, J. W. *Org. Lett.* **2004**, *6*, 1585.

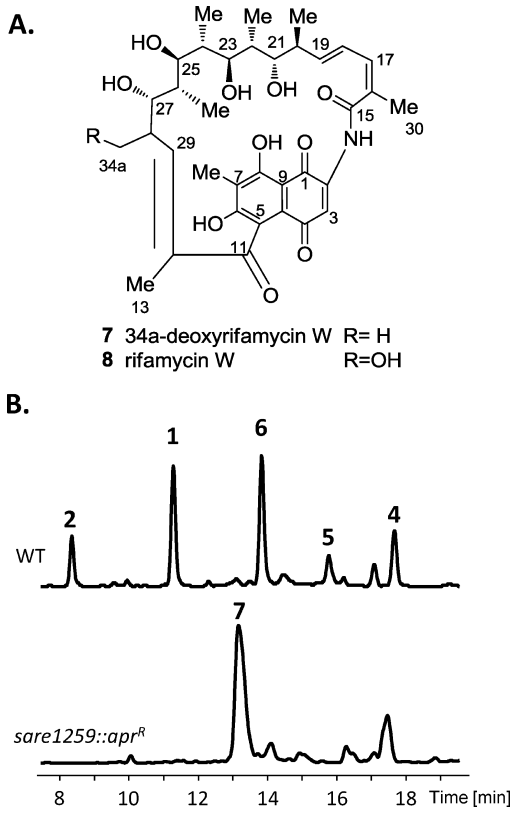

Figure 5. Inactivation of the cytochrome P450, *sare1259*. (A) Structure of rifamycin biosynthetic intermediates 34a-deoxyrifamycin W (**7**) and rifamycin W (**8**). (B) EIC for masses corresponding to the *m/z* of the sodium adducts of the saliniketals (**1**−**2**) and rifamycins (**4**−**8**) produced by *S. arenicola* wild-type and *sare1259::apr*^{R} strains, showing the loss of saliniketal (**1**−**2**) production and accumulation of **7** in the mutant.

of 34a-deoxyrifamycin W (**7**). Importantly, C16/C17 of **1** originate from a propionate unit versus acetate as we originally contemplated.

We next turned our attention to the other three genes with characterized AM-*rif* homologues (*sare1245*, *sare1259*, *and sare1260*) that code for CYPs. Previous inactivation of the CYP *rif-orf16* in *A. mediterranei* S699 produced a mixture of **3** and **4**,[13] and upon further analysis, we showed that this mutation had no effect on the production of **1** and **2**. Similarly, inactivation of the *S. arenicola* homologue, *sare1260* (73% identity), did not alter the production of **1**, **2**, and **4**−**6**.

The CYP encoded by *sare1245* shares 82% identity with *rif-orf0*, and unlike the other *rif* CYPs, they are similarly positioned directly upstream of the rifamycin PKS gene *rifA* rather than in the downstream region that primarily harbors the tailoring and regulatory genes (Figure 3). Lee et al. suggest that the AM *rif-orf0* CYP is responsible for the introduction of the C34a hydroxyl group in rifamycin W (**8**, Figure 5a) based on their observation that inactivation of *rif-orf0* in *A. mediterranei* resulted in a mutant that no longer produced rifamycin B yet accumulated proansamycin X.[24] Our attempt to inactivate the homologous *sare1245* resulted in a mutant that no longer produced either the rifamycins or saliniketals. Subsequent chemical complementation of the *sare1245* mutant (*sare1245::apr*^{R}) with AHBA failed to restore saliniketal/rifamycin production. However, complementation of *sare1245::apr*^{R} with **7** rescued the production of the saliniketals and rifamycins, suggesting that the gene product of *sare1245* is not involved in the post-PKS modification of rifamycin or the biosynthesis of **1** and **2** (Figure S3, Supporting Information). Identical results were observed for the inactivation of the *rifS* (*sare1242*) and *rifT* (*sare1243*) homologues, which are located immediately upstream of *sare1245* on the same putative transcriptional operon. This suggested that inactivation of *rif-orf0*, *rifS*, and *rifT* produced a polar effect on the transcription of the rifamycin polyketide genes, *rifA-F*, directly downstream of *sare1245*, thus resulting in the observed chemotype for all respective mutant strains.

The third and final *SA-rif* CYP *sare1259* is homologous to two *AM-rif* CYPs, namely *orf13* and *orf5*, at 79% and 71% identity, respectively (Table 1). Xu et al. showed, using *in vivo* mutagenesis, that the gene product of *rif-orf*13 in *A. mediterranei* S699 is not involved in rifamycin B (**3**) production, while inactivation of *rif-orf*5 yielded a mutant that accumulated the biosynthetic intermediate rifamycin W (**8**, Figure 5a) in lieu of **3**.[13] The authors concluded that the CYP encoded by *rif-orf5* catalyzes the multistep oxidative conversion of **8** to **6**.[13] Further analysis of the AM-*rif-orf5* mutant in this study, however, revealed that the mutant also produced **1**, **2**, **4**, and **6** as minor components (Figure S4, Supporting Information). With this knowledge in hand, we genetically inactivated *sare1259* in *S. arenicola*. The resulting mutant (*sare1259::apr*^{R}) lost not only the biosynthetic ability to produce rifamycins **4**−**6**, as expected, but significantly the saliniketals as well (Figure 5b). This suggested that the CYP encoded by *sare1259* is a key enzyme in the biosynthesis of **1** and **2** in *S. arenicola* and confirms our hypothesis that the saliniketals are products of an enzymatic cleavage of a rifamycin macrocyclic intermediate versus a shunt product of the polyketide elongation. Interestingly, *sare1259::apr*^{R} accumulated an unexpected product that was confirmed by NMR analysis to be the rifamycin biosynthetic intermediate 34a-deoxyrifamycin W (**7**) instead of the predicted product **8**. The presence of two homologues to *sare1259* in the *AM-rif* pathway may account for the accumulation of **8** in the *AM-rif-orf5* mutant, where the CYP encoded by *rif-orf13* may hydroxylate C34a of **7** and perhaps even perform the conversion of **7** to **1**, **2**, and **6**.

The mechanism proposed for the function of the CYP encoded by *rif-orf5* involves the oxidative cleavage of the C12/C29 double bond followed by rearrangement of the *ansa* chain to form **6** from **8**.[13] If Sare1259 also performs the same oxidative cleavage of the C29/C12 olefin to yield **1**, then C16/C17 of **1** would have to come from an alternate two-carbon source such as the acetate unit in **5** that we previously ruled out. Analysis of the [U−$^{13}C_3$]propionate-labeled **1**, however, unequivocally showed that C15/C16/C17 originates from an intact propionate molecule, thereby suggesting that this three-carbon unit is most likely derived from C12/C13/C29 in **7** (Figure 4). Consequently, these data suggest that Sare1259 has dual function to oxidatively cleave **7** at the C12/C29 olefin to yield the rifamycins and at the C11/C12 bond to give the saliniketals. The biosynthesis of **2** may similarly proceed from a 30-hydroxyrifamycin W precursor, which was previously observed in a recombinant strain of *A. mediterranei*,[25] to account for its C18 hydroxyl group.

In order to determine if any gene products other than the CYP encoded by *sare1259* are also necessary for the biosyn-

(24) Lee, S. K.; Choi, C. Y.; Ahn, J. S.; Cho, J. Y.; Park, C. S.; Yoon, Y. J. *J. Microbiol. Biotechnol.* **2004**, *14*, 356.

(25) Schupp, T.; Traxler, P.; Auden, J. A. *J. Antibiot. (Tokyo)* **1981**, *34*, 965.

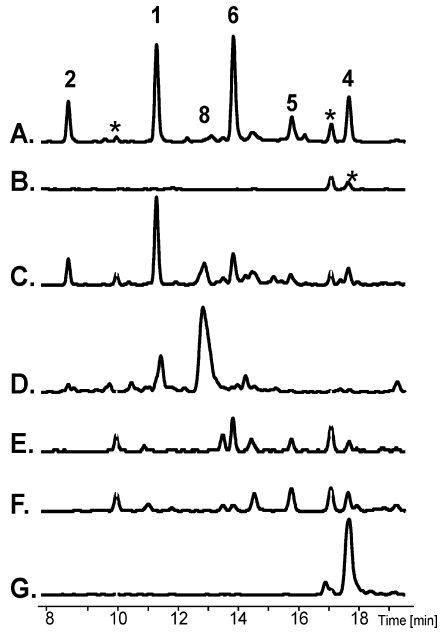

Figure 6. HPLC-MS analysis of the chemical complementation of *rifK::apr*^{R} with rifamycin biosynthetic intermediates. EIC for all masses corresponding to the *m/z* of the sodium adducts of the saliniketals (**1**−**2**) and rifamycins (**3**−**8**) for (A) wild-type *S. arenicola* CNS-205, (B) *rifK::apr*^{R} negative control, (C) *rifK::apr*^{R} complemented with **7**, (D) *rifK::apr*^{R} complemented with **8**, (E) *rifK::apr*^{R} complemented with **6**, (F) *rifK::apr*^{R} complemented with **5**, and (G) *rifK::apr*^{R} complemented with **4** (* indicates unrelated compounds that share an *m/z* ratio with one of the compounds **1**−**8**).

thesis of **1**, an additional eight genes (*sare1242*, *sare1243*, *sare1263*−*sare1267*, and *sare1274*), for which no function has been either confirmed or evaluated in *A. mediterranei* (Table 1), were inactivated in *S. arenicola*. While inactivation of *sare1242* (*rifS*) and *sare1243* (*rifT*) created putative polar effects on the downstream PKS resulting in the total loss of rifamycin/saliniketal biosynthesis, inactivation of the six remaining genes in either *S. arenicola* CNS-205 (this study) or *A. mediterranei* S699 (see ref 13) had no effect on the biosynthesis of **1**−**8** (Figure S2, Supporting Information).

Chemical Complementation of the *rifK* Mutant with Rifamycin Macrocyclic Intermediates. In order to confirm **7** as an immediate precursor to the saliniketals, we complemented cultures of *rifK::apr*^{R} with successive biosynthetic intermediates from the rifamycin pathway **7** → **8** → **6** → **5** → **4**. Complementation with both **7** and **8** enabled restored production of the saliniketals, while intermediates **4**−**6** did not rescue their production (Figure 6). While the complementation of *rifK*::*apr*^{R} with **8** was able to restore saliniketal production, the bioconversion of **8** to **1** and **2** does not appear to be as efficient as the conversion of **7** to **1** and **2** (Figure 6C and D). These findings support our mutagenesis results indicating that the saliniketals are synthesized during the bioconversion of **7** to **6** by Sare1259 with **8** as a potential intermediate. The intermediates that were not able to rescue saliniketal production are presumed to be taken up by the cells based on the observation that the early biosynthetic intermediates can undergo bioconversion into later stage rifamycins (Figure 6C−E).

Discussion

The great structural diversity of naturally occurring rifamycins is largely due to the extensive post-PKS enzymatic tailoring carried out by enzymes encoded by pathway specific genes. After more than 50 years of study, the rifamycin pathway continues to reveal new and unusual biosynthetic potential. The saliniketals are another example of how enzymatic tailoring of natural products by CYPs can produce novel chemical structures through complex chemical reactions.

CYPs are known to catalyze a multitude of diverse oxidative modifications (e.g., hydroxylation, epoxidation, oxidative bond cleavage, or dehydrogenation) on a wide range of molecular substrates, often activating or detoxifying the chemical species.[26−28] The CYP encoded by *sare1259* is most closely related to *rif-orf13* and *rif-orf5* from the AM-*rif* cluster as well as other CYPs belonging to the CYP107 family. This superfamily includes a large number of bacterial CYPs, many of which are associated with xenobiotic degradation and secondary metabolite tailoring.[29−32]

Our data suggest that Sare1259 catalyzes multiple oxidations of **7** at variable positions for its conversion to either the saliniketals or rifamycins. During the biosynthesis of **3**, C34a of **7** is proposed to be sequentially oxidized twice and then lost via a decarboxylation of the resulting carboxyl.[13,33] We hypothesize that the timing of this decarboxylation reaction determines whether the final product of the SA-*rif* pathway yields the rifamycins (**3**−**6**) or the saliniketals (**1**−**2**). The current mechanism proposed for the function of the CYP encoded by *rif-orf5* in *A. mediterranei* involves the oxidative cleavage of the C12/C29 double bond of **7** followed by formation of the ketal of **6** and decarboxylation of the C34a carboxyl group.[13] In contrast, for the production of **1** and **2**, we propose that the decarboxylation reaction occurs prior to oxidative bond cleavage, shifting the C12/C29 olefin to the C11/C12 position where it is then cleaved in a similar fashion by Sare1259 (Figure 7). Reduction of the resulting C28/C29 olefin and rearrangement of the ansa chain would form the 5-carboxy intermediate of the salinisporamycin A (**10**), a recently described compound isolated from *S. arenicola* YM23-082.[34] Our proposed mechanism is further supported by the [U−$^{13}C_3$]propionate tracer experiments and by the isolation of (5-carboxy)salinisporamycin A from fermentations of *S. arenicola* (J. B. MacMillan, personal communication). The isolation of **10** by Matsuda and co-workers also suggests the sequence of transformation from **7** to **1** proceeds with the formation of the bicyclic ketal prior to the construction of the primary amide. Mechanisms for this latter reaction may involve an oxidation of the quinone at C2 or reduction of the quinone to the hydroquinone followed by a retro-Michael cleavage of the C−N bond to yield **1** and the respective naphthoquinone (Figure 7). Attempts to identify and isolate the resulting naphthoquinone moiety have thus far been unsuccessful. Additionally, we did not identify a *rif* pathway gene associated with the putative conversion of (5-carboxy)-

(26) O'Keefe, D.; Harder, P. *Mol. Microbiol.* **1991**, *5*, 2099.
(27) Meunier, B.; de Visser, S. P.; Shaik, S. *Chem. Rev.* **2004**, *104*, 3947.
(28) Guengerich, F. P. *Chem. Res. Toxicol.* **2008**, *21*, 70.
(29) Weber, J. M.; Leung, J. O.; Swanson, S. J.; Idler, K. B.; McAlpine, J. B. *Science* **1991**, *252*, 114.
(30) Trefzer, A.; et al. *Appl. Environ. Microbiol.* **2007**, *73*, 4317.
(31) Fujii, Y.; Kabumoto, H.; Nishimura, K.; Fujii, T.; Yanai, S.; Takeda, K.; Tamura, N.; Arisawa, A.; Tamura, T. *Biochem. Biophys. Res. Commun.* **2009**, *385*, 170.
(32) Prior, J. E.; Shokati, T.; Christians, U.; Gill, R. T. *Appl. Microbiol. Biotechnol.* **2010**, *85*, 625.
(33) Traxler, P.; Schupp, T.; Fuhrer, H.; Richter, W. J. *J. Antibiot. (Tokyo)* **1981**, *34*, 971.
(34) Matsuda, S.; Adachi, K.; Matsuo, Y.; Nukina, M.; Shizuri, Y. *J. Antibiot. (Tokyo)* **2009**, *62*, 519.

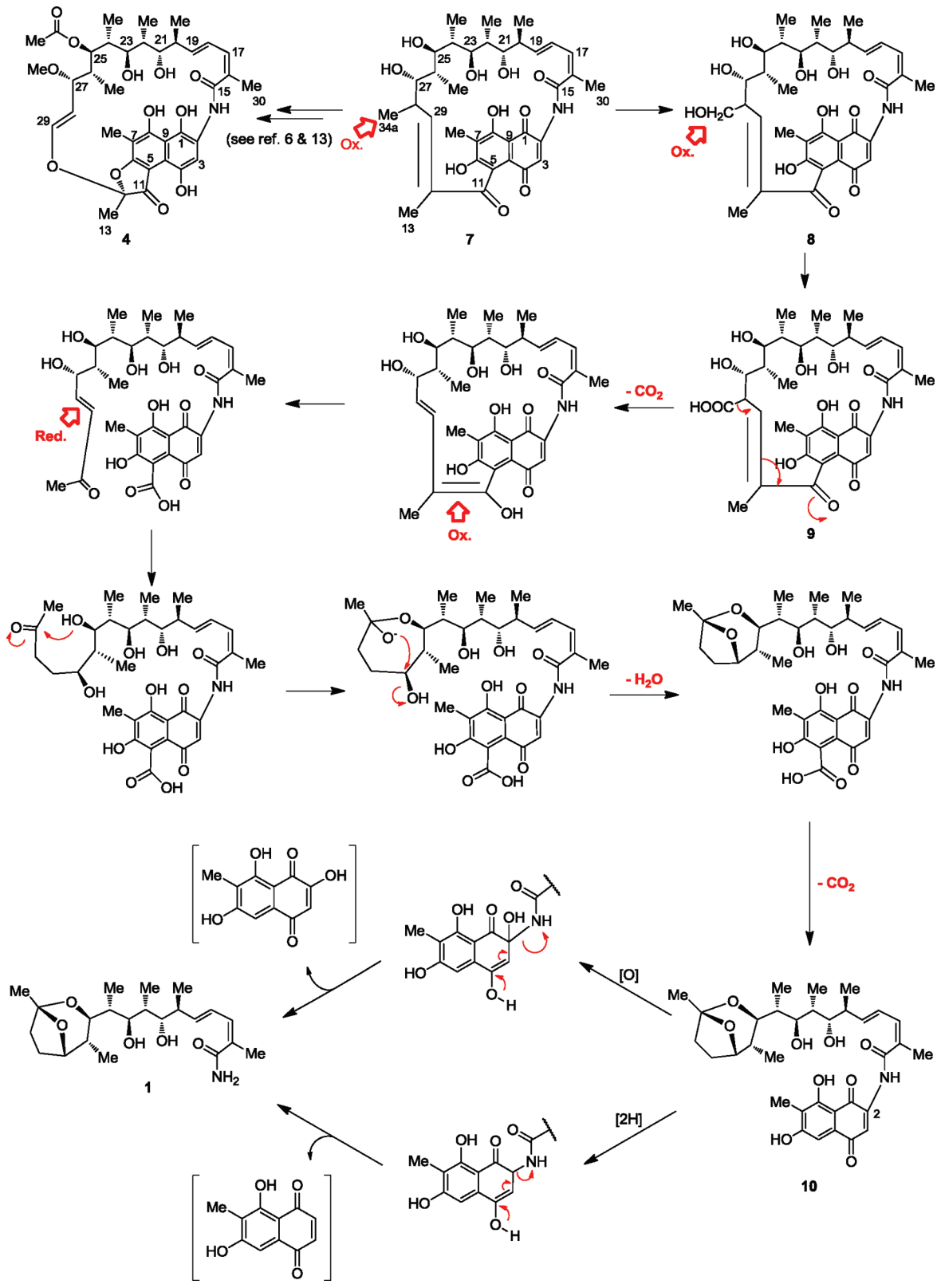

Figure 7. Proposed mechanism of saliniketal biosynthesis facilitated by CYP Sare1259 (intermediates with published structures are numbered).[1,25,33,34]

salinisporamycin A to **1**, which may suggest that if this reaction is indeed catalyzed by a dedicated enzyme, it may be encoded outside the *rif* cluster.

In conclusion, we took a multidisciplinary approach involving a combination of genomics, in vivo mutagenesis, chemical complementation, stable isotope incorporation studies, and chemical analyses to interrogate the biosynthetic origin of the saliniketals. Such a multifaceted approach was required to effectively explore the biosynthesis of the saliniketals that ultimately led to the identification of the Sare1259 CYP as the key biosynthetic gene product that governs the diversification of the *rif* pathway at the stage of 34a-deoxyrifamycin W (**7**)

leading to the truncated saliniketals and mature rifamycins (Figure 7). We are presently probing the multifunctional Sare1259 to explore its preferred substrates, its reaction profile, and its molecular mechanism that likely will lead to new P450 catalyzed chemistry.

Experimental Section

General Methods. Low-resolution LC/MS was carried out on a Hewlett-Packard series 1100 LC/MS system in positive ion mode with a linear gradient of 10−90% MeCN at a flow rate of 0.7 mL/min over 24 min on an RP C_{18} column (Phenomenex Luna, 4.6 mm ×100 mm, 5 μm). ^{1}H, heteronuclear multiple bond correlation (gHMBC) and heteronuclear single quantum coherence (gHSQC) NMR spectral data were obtained on a Bruker DRX600 spectrophotometer equipped with a 1.7 mm cryoprobe. ^{13}C NMR spectral data were obtained on a Varian VX-500 instrument equipped with an XSens cold probe. Rifamycin SV (**4**) sodium salt was purchased from Sigma Aldrich (St. Louis, MO). Saliniketal A (**1**) was graciously provided by William H. Fenical.[1] Rifamycin W (**7**), 27-*O*-demethyl-24-*O*-desacetylrifamycin SV (**6**, DMDARSV), and 27-*O*-demethylrifamycin SV (**5**, DMRSV) were isolated and confirmed based on literature precedence.[13,16,17]

Bacterial Strains, Culture Conditions, and Extraction of Natural Products. *Salinispora arenicola* strain CNS-205 and *Amycolatopsis mediterranei* strains S699, MT45025H, and MT1601KH were obtained as described previously.[13,20] All *S. arenicola* seed cultures were grown in A1 liquid media (10 g of starch, 5 g of yeast extract, and 2 g of peptone per liter of seawater), and production cultures were grown in A1BFeC liquid media (10 g of starch, 5 g of yeast extract, 2 g of peptone, 100 mg of KBr, 40 mg of $Fe_2(SO_4)_3 \cdot 4H_2O$, 1 g of $CaCO_3$ per 1 L of seawater) at 28 °C and 225 rpm.[20] *Amycolatopsis mediterranei* S699 seed and production cultures were both grown in YMG liquid media[35] at 28 °C and 225 rpm, unless otherwise noted. Extraction of saliniketal and rifamycin compounds was achieved by acidifying the culture broth to pH 2−3 with 1 N HCl and extracting the cultures 3× with equal volumes of EtOAc. The organic fraction was dried under vacuum, resuspended in MeOH, and analyzed by LC/MS. *Escherichia coli* strains EPI300, BW25113/pKD20,[36] and S17-1[37] used for mutagenesis experiments were grown in Luria-Bertani (LB) media with appropriate antibiotics.

Genetic Manipulations. Inactivation of rifamycin and saliniketal biosynthetic genes was performed using REDIRECT PCR targeting technology as described previously for *S. arenicola*.[20,38] *E. coli* EPI300 (Epicenter) carrying fosmids BPPW5227, BPAF1230, and BPAF1361 were provided by the Joint Genome Institute, Walnut Creek, CA. Each of the genes targeted for inactivation was replaced with an apramycin resistance (*acc(3)IV*) cassette by double crossover homologous recombination on the fosmid containing the gene of interest. The mutant fosmid was then transformed into *E. coli* S17-1 and transferred to *S. arenicola* CNS-205 via conjugation. Exconjugates were confirmed by PCR analysis and restriction digest.

Isolation of 34a-Deoxyrifamycin W (7) from the *sare1259::apr^R* Mutant. The *sare1259::apr^R* mutant was cultured in 8 × 1 L Fernbach flasks of A1BFeC media for 7 days at 28 °C while shaking at 225 rpm. XAD-7 resin (30 g) was added to each flask on day 7 and continued to shake for 5 h before collecting the resin by filtration. The resin was then extracted with 3 × 1 L of acetone and concentrated under vacuum. The residue was separated by silica gel flash chromatography under isocratic conditions with MeOH/$CHCl_3$ (1:9). Silica fractions were further purified by HPLC on an RP C_{18} column (Phenomenex Luna, 10 mm ×250 mm, 5 μm, MeCN/H_2O 56:44, v/v).

34a-Deoxyrifamycin W (7). HPLC ESI-MS: $[M + Na]^+$ 662.3; ^{1}H NMR (600 MHz, DMSO-d_6) δ 12.40 (s, 8-OH), 10.54 (br s, 6-OH), 9.59 (s, NH), 7.47 (s, H-3), 6.32 (dd, J = 15.5, 11.2 Hz, H-18), 6.16 (d, J = 10.8 Hz, H-17), 5.99 (dd, J = 15.6, 6.9 Hz, H-19), 4.76 (d, J = 6.5 Hz, 23-OH), 4.35 (s, 21-OH), 4.31 (d, J = 5.8 Hz, 27-OH), 3.84 (d, J = 5.6 Hz, H-27), 3.80−3.73 (m, H-25), 3.68 (d, J = 6.5 Hz, 25-OH), 3.35−3.28 (m, H-23), 2.40 (dd, J = 15.1, 7.3 Hz, H-28), 2.20 (dd, J = 14.6, 7.2 Hz, H-20), 2.13 (s, H-14), 2.00 (s, H-30), 1.89 (s, H-13), 1.65 (br d, J = 6.8 Hz, H-22), 1.59−1.51 (m, H-24), 1.25−1.15 (m, H-26), 0.95 (d, J = 7.0 Hz, H-34a), 0.91 (d, J = 6.9 Hz, H-32), 0.81 (d, J = 6.8 Hz, H-31), 0.55 (d, J = 6.7 Hz, H-33), 0.18 (d, J = 6.9 Hz, H-34).

Chemical Complementation of *S. arenicola* Mutants. Chemical complementation studies were carried out in 50 mL cultures of the *S. arenicola rifK::apr^R* mutant in A1 production media. Compounds **4**−**8** (2−6 mg) were individually added in triplicate to 1 day old production cultures of *rifK::apr^R*. The cultures were then allowed to grow for 4 more days before being extracted as described above. Bioconversion of the rifamycin intermediates was monitored by HPLC-MS. Retention times, *m/z* ratios, and UV profiles of the biotransformation products were compared to authentic standards.

Synthesis of ^{15}N-AHBA. AHBA was synthesized by reacting 3,5-dihydroxybenzoic acid (2.0 g, 13 mmol) with NH_4Cl (1.7 g, 32 mmol) and aqueous NH_4OH (14.8N, 6 mL, 89 mmol) in a sealed high-pressure reaction tube at 180 °C for 40 h.[39,40] After cooling, the volatile components of the reaction mixture were removed in vacuo and the remaining solid was redissolved in 100 mL of 6 N HCl. The resulting solution was heated under reflux for 16 h, filtered, extracted with EtOAc (3 × 40 mL) to remove unreacted starting material, and concentrated to 25 mL. The desired product crystallized from this solution yielding gray crystals, which were collected and recrystallized from 6 N HCl to furnish pure AHBA hydrochloride as white crystals in 68% overall yield (1.67 g, 8.8 mmol). The [^{15}N]AHBA was prepared following the same synthetic route but substituting NH_4Cl with $^{15}NH_4Cl$. The statistically expected ^{15}N-enrichment of 25% in the product was verified by mass spectrometric analysis. ^{1}H NMR (500 MHz, CD_3OD) δ 7.04 (m, 1H), 7.48 (m, 1H), 7.51 (m, 1H). HPLC ESI-MS: AHBA $[M + H]^+$ 154.1; [^{15}N]AHBA $[M + H]^+$ 154.1 (75%), 155.2 (25%).

Stable Isotope Labeling Experiments of 1. [U-$^{13}C_3$]Propionate incorporation experiments were carried out in 2 × 1 L cultures of *S. arenicola* CNS-205 grown in A1BFeC liquid media at 225 rpm and 30 °C for 7 days. Sodium [U-$^{13}C_3$]propionate (50 mg/L) (Cambridge Isotopes Laboratories, Incorporated) was aseptically added to each liter of culture after 48 h. The cultures were extracted with EtOAc, and **1** was isolated as described previously[1] and analyzed by ^{13}C NMR (Figures S5 and S6, Supporting Information). [^{15}N]AHBA incorporation studies were carried out in 50 mL cultures of *rifK::apr^R* in A1BFeC at 225 rpm and 30 °C for 5 days. [^{15}N]AHBA (3 mg) was added to each culture after 24 h and extracted as described above on day five. Crude extracts were analyzed by HPLC-MS. Incorporation of ^{15}N into AHBA and **1** was calculated from *m/z*.[41] HPLC ESI-MS: saliniketal A (**1**) $[M + Na]^+$ 418.3; [^{15}N]saliniketal A (**1**) $[M + Na]^+$ 418.2 (75%), $[M + Na]^+$ 419.2 (25%).

Acknowledgment. We thank William H. Fenical and Paul R. Jensen for kindly providing authentic standards of saliniketal A

(35) Kim, C. G.; Yu, T. W.; Fryhle, C. B.; Handa, S.; Floss, H. G. *J. Biol. Chem.* **1998**, *273*, 6030.
(36) Datsenko, K. A.; Wanner, B. L. *Proc. Natl. Acad. Sci. U.S.A.* **2000**, *97*, 6640.
(37) Simon, R.; Priefer, U.; Puhler, A. *Bio-Technol* **1983**, *1*, 784.
(38) Gust, B.; Challis, G. L.; Fowler, K.; Kieser, T.; Chater, K. F. *Proc. Natl. Acad. Sci. U.S.A.* **2003**, *100*, 1541.
(39) Becker, A. M.; Rickards, R. W.; Brown, R. F. C. *Tetrahedron* **1983**, *39*, 4189.
(40) Wang, Z.; Silverman, R. B. *Bioorg. Med. Chem.* **2006**, *14*, 2242.
(41) Biemann, K. *Mass spectrometry: organic chemical applications*; McGraw-Hill: New York, 1962.
(42) Oppolzer, W.; Prelog, V.; Sensi, P. *Experientia* **1964**, *20*, 336.
(43) White, R. J.; Martinelli, E.; Lancini, G. *Proc. Natl. Acad. Sci. U.S.A.* **1974**, *71*, 3260.

(**1**) and *S. arenicola* CNS-205, respectively. We also thank Heinz G. Floss for his comments and assistance in the preparation of this manuscript. This work was generously supported by a grant from the NIH (GM085770 to B.S.M.) and a postdoctoral fellowship from the German Academic Exchange Service (DAAD) to T.A.M.G.

Supporting Information Available: HPLC-MS spectra for *A. mediterranei* S699 and *rif-orf5* mutant strain, HPLC-MS spectra for SA-*rif* mutants generated in this study, HPLC-MS spectra for *sare1245::apr*^{R} chemical complementation study, ^{13}C NMR spectra for ^{13}C-labeled **1**, 1D and 2D NMR spectra (^{1}H, gHSQC, gHMBC) for **7**, table of primers used in this study, and complete ref 30. This material is available free of charge via the Internet at http://pubs.acs.org.

JA105891A